

Ordered Structure in Blends of Block Copolymers. 2. Self-Assembly for Immiscible Lamella-Forming Copolymers

Takeji Hashimoto,* Satoshi Koizumi, and Hirokazu Hasegawa

*Division of Polymer Chemistry, Graduate School of Engineering, Kyoto University,
Kyoto 606, Japan*

*Received August 16, 1993; Revised Manuscript Received November 30, 1993**

ABSTRACT: The self-assembly of binary mixtures of poly(styrene-block-isoprene) was investigated by small-angle X-ray scattering and transmission electron microscopy. The copolymers investigated had nearly equal compositions of styrene and isoprene but different molecular weights such that each copolymer by itself forms lamellar microdomains in the segregation limit. The mixtures, however, underwent macroscopic phase separation into domains rich in large and small molecular weight copolymers, both forming the lamellar microdomain in the segregation limit. Interesting commensurations were formed at the macroscopic interface of the two domains composed of thick and thin lamellae. A possible interpretation of the macrophase separation was proposed on the basis of the *macrophase separation induced by the microphase separation*.

I. Introduction

Binary mixtures $(A-B)_\alpha/(A-B)_\beta$ of A-B type diblock copolymers, having different total degrees of polymerization N_α and N_β and compositions $f_{\alpha,A}$ and $f_{\beta,A}$ of A block chains can generally have two kinds of phase transition, i.e., microphase transition of A and B block chains in the block copolymers and macrophase transition between two polymers, $(A-B)_\alpha$ and $(A-B)_\beta$. Hereafter we designate $(A-B)_\alpha$ and $(A-B)_\beta$ as copolymers α and β for the sake of convenience. A coupling or interplay of the two kinds of phase transition will give rich varieties in their self-assembling processes, mechanisms, and patterns.¹ These mixtures involve problems similar to those of A-B/A and A-B/A/B as pointed out previously,² where A and B designate A and B homopolymers, respectively. However, the mixture $(A-B)_\alpha/(A-B)_\beta$ involves a greater degree of constraint than mixtures with homopolymers in a strong segregation limit in that the former invokes a strong localization of the center of mass of two copolymers somewhere in the domain space, because the chemical junctions must be located near interfaces, while the latter invokes a weaker localization, as the center of mass of homopolymers A and/or B can be somewhere in the corresponding microdomains. The smaller translational entropy of the former makes a greater contribution of the elastic free energy associated with the coil stretching³⁻⁷ in the microdomain space, compared with that of the latter.

In part 1 of this work,² we found that two copolymers α and β of similar compositions ($f_{\alpha,A} \approx f_{\beta,A}$) but disparate degrees of polymerization ($N_\alpha/N_\beta > 10$) show only a partial miscibility. They do not mix with each other at the molecular level but undergo macrophase separation into the domains rich in copolymers α and those rich in copolymers β when the composition of α in the mixtures, ϕ_α is $\phi_{\alpha,c}^S < \phi_\alpha < \phi_{\alpha,c}^L$ (Figure 1b). Here the compositions $\phi_{\alpha,c}^S$ and $\phi_{\alpha,c}^L$ are respectively the critical compositions, below and above which the two copolymers are mixed molecularly in the same domains without macrophase separation (Figure 1c). We also found that the larger molecular weight copolymers α can incorporate the smaller molecular weight copolymers β in their domains, up to about 30 vol %, i.e.

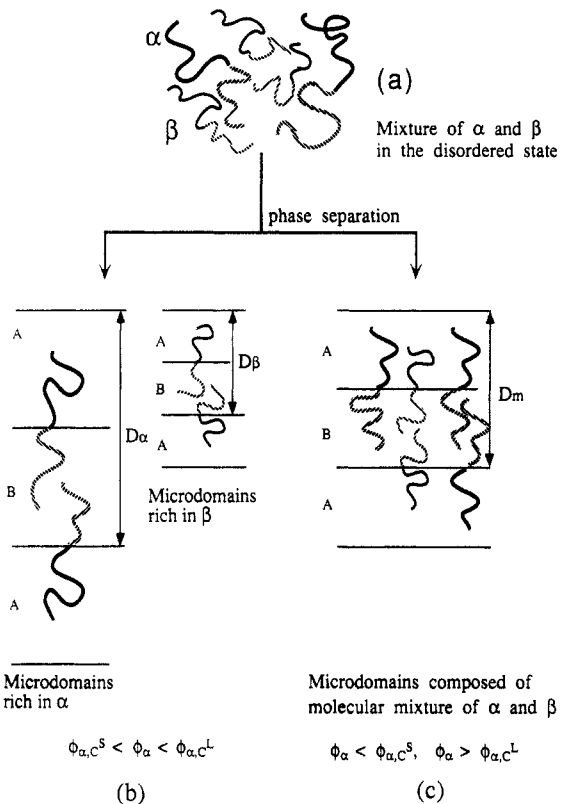


Figure 1. Summary of the possible ordered structures for the binary mixtures of block copolymers α/β with $f_{\alpha,A} \approx f_{\beta,A} \approx 0.5$ but $r = N_\alpha/N_\beta > 10$: (a) α and β mixed in the disordered state; (b) macrophase separation into the microdomains rich in α and the microdomains rich in β ; (c) single microdomain structure in which α and β are mixed uniformly.

$$\phi_{\alpha,c}^L \approx 0.7 \quad (1)$$

as typically shown in Figure 2, where the lamellar domain spacings as observed by small-angle X-ray scattering (SAXS) are plotted as a function of ϕ_α . The critical composition $\phi_{\alpha,c}^S$ appears to be very low, indicating that the thinner lamellar domains dominantly composed of the β copolymers can hardly incorporate the large copolymers α , i.e., the β -rich lamellar domains are almost pure with β . The critical compositions $\phi_{\alpha,c}^L$ and $\phi_{\alpha,c}^S$ were expected to be closely related to the elastic free energy of copolymers α and β when they are packed in the same domains with their junctions at the interface. The macrophase separation was proposed to occur as a con-

* Abstract published in Advance ACS Abstracts, February 1, 1994.

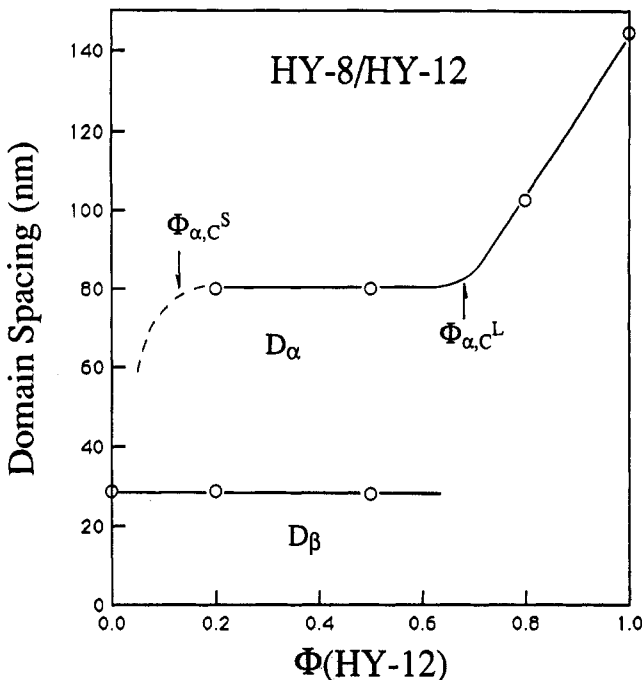


Figure 2. Plots of the average domain spacings for HY-8/HY-12 as a function of the weight fraction of block copolymers α (HY-12). The mixture shows a partial miscibility forming the two coexisting macrophases of the lamellae having large and small spacings, D_α and D_β , respectively, in the composition range between the critical concentrations $\phi_{\alpha,c}^S$ and $\phi_{\alpha,c}^L$.

sequence of the microphase separation,² i.e., "macrophase separation induced by the microphase separation".

In this work we explore self-assembly of the mixtures in the criterion where the mixtures undergo macrophase separation. We investigate the morphology of the mixtures as studied by transmission electron microscopy (TEM). We will propose the *fluctuation-induced segregation* effect as a possible picture which accounts for macrophase separation (see section IV.B).

II. Experimental Section

Poly(styrene-block-isoprene) copolymers (SI) used in this work were synthesized by living anionic polymerization. For all the details regarding the synthesis of the copolymers, preparation of the blend specimens, and SAXS and TEM analyses, refer to part 1 of this series.² Table 1 shows characteristics of the copolymers used in this work. The blends studied in this work are HK-17/HS-10, HS-10/HS-9, and HY-8/HY-12, all of which showed only a partial miscibility and macrophase separation in the composition range satisfying $\phi_{\alpha,c}^S < \phi_\alpha < \phi_{\alpha,c}^L$.

It will be useful to comment here on the Flory-Huggins interaction parameter χ_{SI} between polystyrene (PS) and polyisoprene (PI) block chains in order to judge the thermodynamic stability of the mixtures α/β for microphase and macrophase transitions. The value χ_{SI} is of order of 0.1 in the usual temperature range of our interests (see, for example, ref 11). This value χ_{SI} should be compared with the χ_{SI} value at the spinodal point for microphase transition, $\chi_{s,\text{micro}}$ and that for macrophase transition, $\chi_{s,\text{macro}}$. The data for $\chi_{s,\text{micro}}$ and $\chi_{s,\text{macro}}$ for our mixtures α/β are summarized in Figure 13, as will be discussed later. The comparisons of χ_{SI} with $\chi_{s,\text{micro}}$ and $\chi_{s,\text{macro}}$ clearly show that $\chi_{s,\text{micro}} < \chi_{SI} \ll \chi_{s,\text{macro}}$: the mixtures should be stable for macrophase transition (i.e., the disordered mixtures α/β should not undergo macrophase transition) but unstable for microphase transition (i.e., the disordered mixtures undergo microphase transition).

III. Experimental Results

Figure 3 shows typical TEM micrographs showing closeups of the macroscopic interface between two coexisting macrodomains. The micrographs were obtained with ultrathin sections of HY-8/HY-12 50/50 w/w stained with OsO₄ so that the bright and dark phases correspond

to the unstained polystyrene (PS) and stained polyisoprene (PI) microdomains, respectively. The upper-left and lower-right halves of Figure 3a and the lower and upper halves of Figure 3b correspond, respectively, to the domains rich in copolymers β (HY-8) and α (HY-12).

Here we should note the beautiful commensuration of the two lamellae having different sizes at the macroscopic interfaces: the thin PS and PI lamellae are continuously connected respectively to the thick PS and PI lamellae with the inclination in one direction ("one-side inclination") at the interface as seen in Figure 3a, without intersecting the unlike domains at the macrointerface. Figure 3b shows other types of commensurations which are frequently found and which also compensate the difference of the domain sizes, while keeping the continuity of the respective domains at the interface: these are the "V-shaped" commensuration made by the inclination in both directions as seen in the region marked V and the "U-Shaped" commensuration in which the thinner lamellae make "hairpin" turns or "U-turns" at the interface as seen in the region marked by U.

It should also be noted that Figure 3b shows interesting topological interfaces called Scherk's first surface⁸ within the domains rich in copolymers α and β , as seen in the regions marked by S. These images correspond to Scherk's first surface viewed at $\theta = 30^\circ$ and $\phi = 30-40^\circ$ in Figure 4 of ref 9. These topological interfaces are generated in the grains where the lamellar domains of different orientations meet each other and can be described on the basis of Scherk's first surface. Figure 4 shows a wire frame model of Scherk's first surface produced by computer graphics^{9,10} (part a). This surface is produced at the grain boundary where two sets of lamellar microdomains with identical spacings meet as shown in part b. The Cartesian coordinate $oxyz$ is taken in such a way that the ox and oy axes are parallel to the unit vector along the lamellar normals \mathbf{l}_1 and \mathbf{l}_2 and the oz axis is normal to the topological interface in the oxy plane. The unit vector \mathbf{n} defines the direction normal to the ultrathin section prepared for the TEM observation, and its orientation with respect to the Cartesian coordinate $oxyz$ is defined by θ and ϕ (part c). Through this Scherk's first surface, the PS and PI lamellae having different orientations can be continuously connected in the grain boundary regions to the respective lamellae without intersecting unlike domains. Hence, Scherk's first surface makes the lamellar domains continuous in 3D space.

We note that there are other types of possible commensurations, an example of which is shown in Figure 5a for HY-8/HY-12: "inverted V-shaped" commensuration as seen in the region marked A which is just opposite to the V-shaped commensuration shown in Figure 3b. Figure 5b shows a macroscopic interface observed for another mixture HS-10/HS-9 80/20 w/w. In contrast to the other case shown above in Figures 3 and 5a, the macroscopic interface does not show the commensurations as described above; the thick PI lamellae are not continuously linked to the thin PI lamellae but are orthogonally intersecting the PS lamellae composed of PS block chains of large and small molecular weight copolymers. The tips of the thick PI lamellae show an interesting arch-type shape.

Figure 6 shows another type of commensuration observed for HY-8/HY-12 50/50 w/w which possibly corresponds to Scherk's first surface made by two orthogonal sets of lamellae with different thicknesses as shown in part c in its wire frame representation. In the TEM micrograph shown in part a, thin bright PS lamellae and dark PI lamellae of copolymers β appear at first glance to intersect thick lamellae of copolymers α . However, a close

Table 1. Characteristics of Poly(styrene-block-isoprene) Used in This Work

specimen code	$M_n \times 10^{-3}$ ^a	M_w/M_n ^b	N_{PS}^c	N_{PI}^d	r_{PS}^e	r_{PI}^f	f_{PS}^g
HK-17	8.5	1.25	40.8	62.4	47.0	54.2	0.46
HY-8	31.6	1.07	146	241	168	209	0.45
HS-10	81.4	1.13	492	442	557	384	0.60
HY-12	524	1.16	2470	3920	2840	3410	0.46
HS-9	1030	1.62	5140	7260	5920	6300	0.48

^a Osmometry. ^b Size-exclusion chromatography. ^c Number-average degree of polymerization (DP) of a polystyrene block chain (PS). ^d Number-average DP of a polyisoprene block chain (PI). ^e $r_{PS} = N_{PS}(v_{PS}/v_0)$; $v_{PS} = 104/1.053 \text{ cm}^3/\text{mol}$. ^f $r_{PI} = N_{PI}(v_{PI}/v_0)$; $v_{PI} = 68/0.913 \text{ cm}^3/\text{mol}$, $v_0 \equiv (v_{PS}v_{PI})^{1/2}$. ^g $f_{PS} = r_{PS}/(r_{PS} + r_{PI})$, volume fraction of PS in the copolymer.

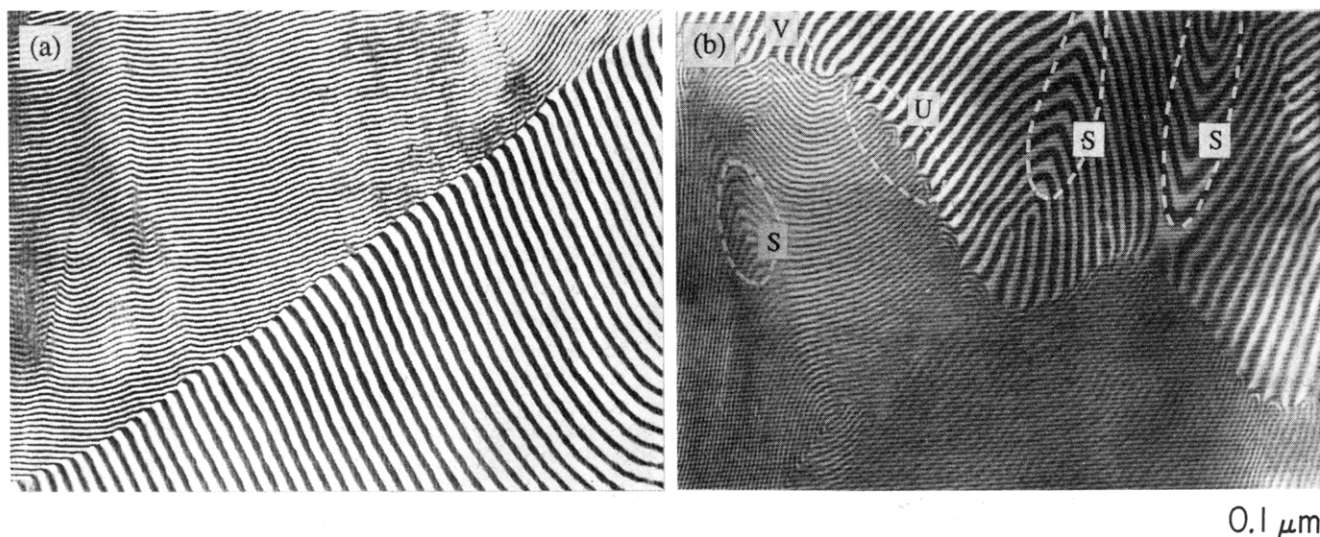


Figure 3. Transmission electron micrographs of ultrathin sections of HY-8/HY-12 50/50 w/w stained by osmium tetroxide. The micrographs focus on the macroscopic interface between the two coexisting macrodomains composed of thick and thin lamellae. Beautiful commensurations are shown in part a (one-side inclination) and in part b (V-shaped and U-shaped commensuration in regions marked V and U, respectively). The regions marked S show the grain boundary as represented by Scherk's first surface.

observation of the micrograph reveals that the thin dark lamellae and thin bright lamellae appear to continuously be connected respectively to the thick dark lamellae and the thick bright lamellae through intervening regions with gray color (i.e., intermediate contrast). The TEM image may correspond to that shown in part b which is simulated for the ultrathin section prepared with the angles $\theta = 50^\circ$ and $\phi = 45^\circ$ and a thickness of one repeat distance of the thick lamellae (part c).

Figure 7 shows a lower magnification of TEM for HY-8/HY-12 50/50 w/w. The darker regions are composed of the thinner lamellae rich in copolymers β , while the brighter regions are composed of the thicker lamellae rich in copolymers α . Figure 8 shows a sketch of TEM micrographs typically seen with a magnification lower than that of Figure 7, again for HY-8/HY-12 50/50 w/w. The macroscopic interface is rigorously drawn in the sketch by tracing the real interface in the micrograph, while the lamellae are ignored in the sketch as they are too thin and are not discernible in this magnification. Figures 7 and 8 elucidate the following important pieces of evidence: (i) the macroscopic interface is very irregular in shape, (ii) the large copolymers α form a continuous phase and the small copolymers β a dispersed phase, and (iii) the lamellar interfaces of the large copolymers α tend to meet the macroscopic interface at angles close to 90° .

Figure 9 shows TEM micrographs for the 80/20 w/w sample of HK-17/HS-10. The micrographs again show macroscopic phase separation between the region rich in copolymers β (HK-17, upper-right half) and the region rich in copolymers α (HS-10). The region rich in copolymers α clearly exhibits the lamellar morphology, while the region rich in copolymers β is featureless, characteristic of the disordered phase in which the PS and PI block

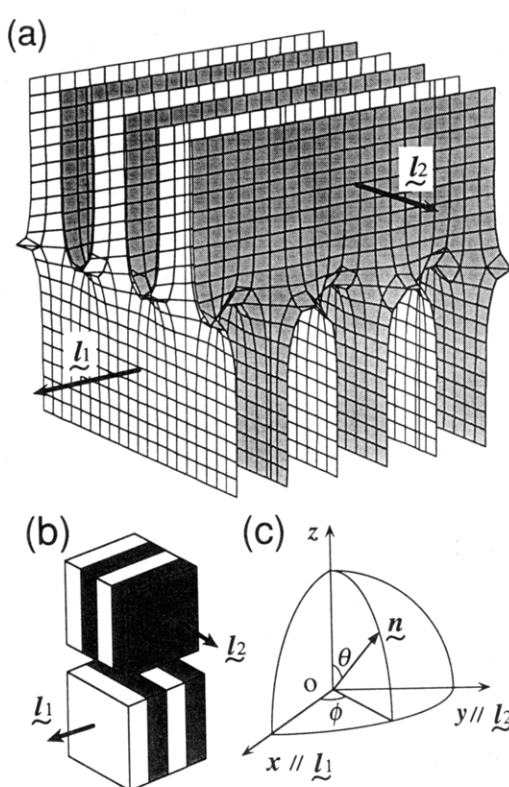


Figure 4. (a) Wire frame model of Scherk's first surface produced by computer graphics. (b) Two sets of orthogonal lamellae with lamellar normals indicated by unit vectors \mathbf{l}_1 and \mathbf{l}_2 ; (c) Orientation of the unit vector \mathbf{n} normal to the thin section with respect to the Cartesian coordinate system fixed to the lamellar system.

chains are molecularly mixed as clarified by the SAXS studies.¹¹

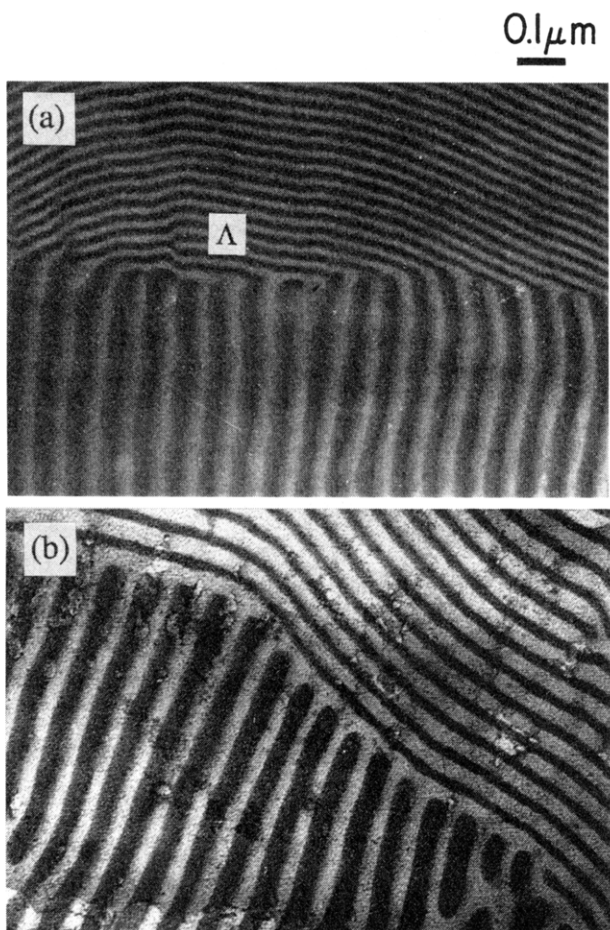


Figure 5. Transmission electron micrographs of ultrathin sections of the binary mixture of (a) HY-8/HY-12 50/50 w/w, showing the “inverted V-shaped” commensuration, and that of (b) HS-10/HS-9 80/20 w/w, showing the intersection of the large PI lamellae with the PS microdomains.

IV. Discussion

A. Commensuration at Macroscopic Interfaces. Figure 10 schematically shows some typical commensurations of the thick and thin lamellae at macroscopic interfaces: (a) one-side inclination, (b) V-shape, (c) inverted V-shape, and (d) U-shape. The macroscopic interface may have the preferred orientation with respect to the lamellar interfaces of the thicker lamellae with thickness D_α in order to minimize the area of the macroscopic interface: it may orient perpendicular to the lamellar interfaces of the thicker lamellae as shown in Figure 10. In either case of the commensurations, the angle κ between the macroscopic interface and the lamellar interface of the thinner lamellae is determined by the ratio of the two lamellar domains,

$$\sin \kappa = D_\beta / D_\alpha \quad (2)$$

Packing the block chains in such a confined space as shown in the hatched region H in Figure 10, i.e., in the lamellar space near the macroscopic interface, may involve elastic deformation of the block chains and hence the excess free energy. This excess free energy contributes to the interfacial tension of such systems.

B. Qualitative Picture of Macrophase Separation Induced by Microphase Separation. We consider here, for example, the 50/50 w/w mixture of copolymers α and β in a neutral solvent such as toluene for the SI copolymers. Microphase separation may occur as the total polymer concentration of the mixture increases to c_1 at a particular time t_1 during the solvent evaporation process. This

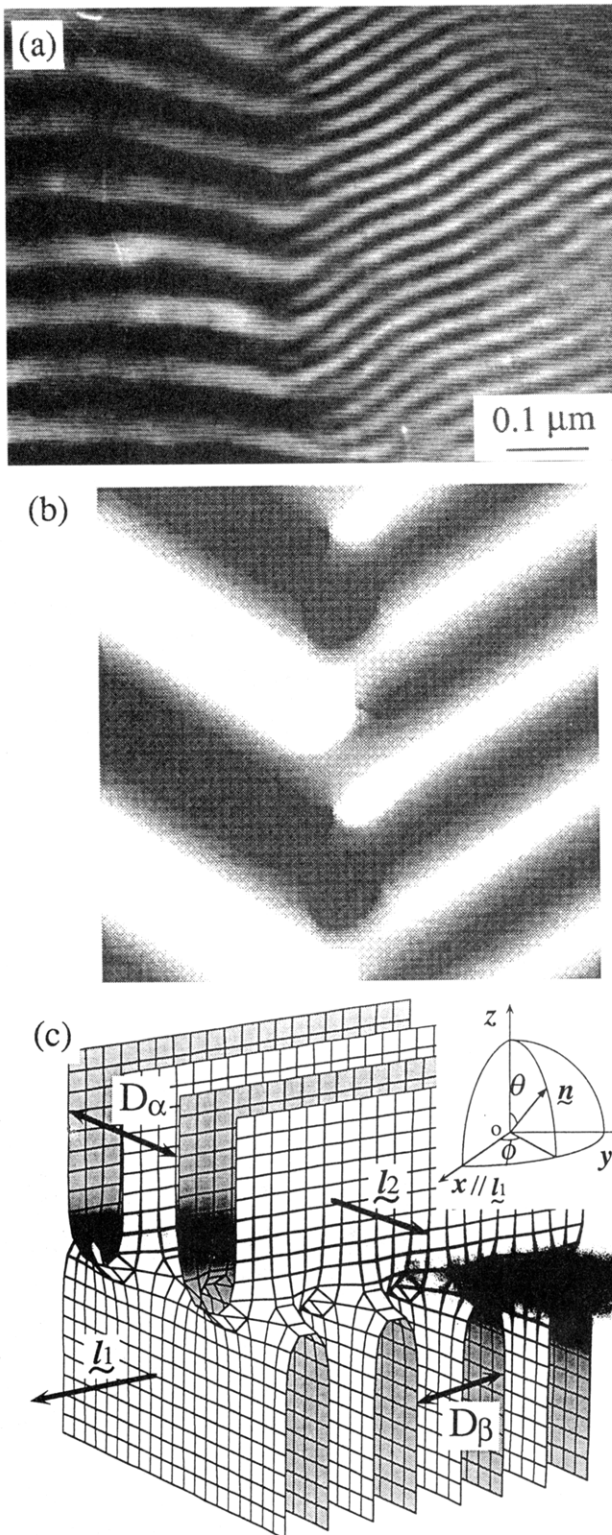


Figure 6. Transmission electron micrographs of HY-8/HY-12 50/50 w/w, showing the commensuration of large and small lamellae at the macroscopic interface through Scherk's first surface (a), a computer-simulated image of the grain boundary through Scherk's first surface obtained for a thin section of thickness D_α (corresponding to one repeat distance of the thick lamellae) oriented at $\theta = 50^\circ$ and $\phi = 45^\circ$ (b), and a wire frame model of Scherk's first surface for two sets of orthogonal lamellae with $D_\alpha/D_\beta = 2$ (D_β being the repeat distance of the thin lamellae) (c). The model c gives the image shown in b.

microphase separation may occur according to the nucleation growth mechanism (NG)¹² or the spinodal decomposition mechanism (SD).¹³ We first consider a possibility of domain growth according to the former mechanism.

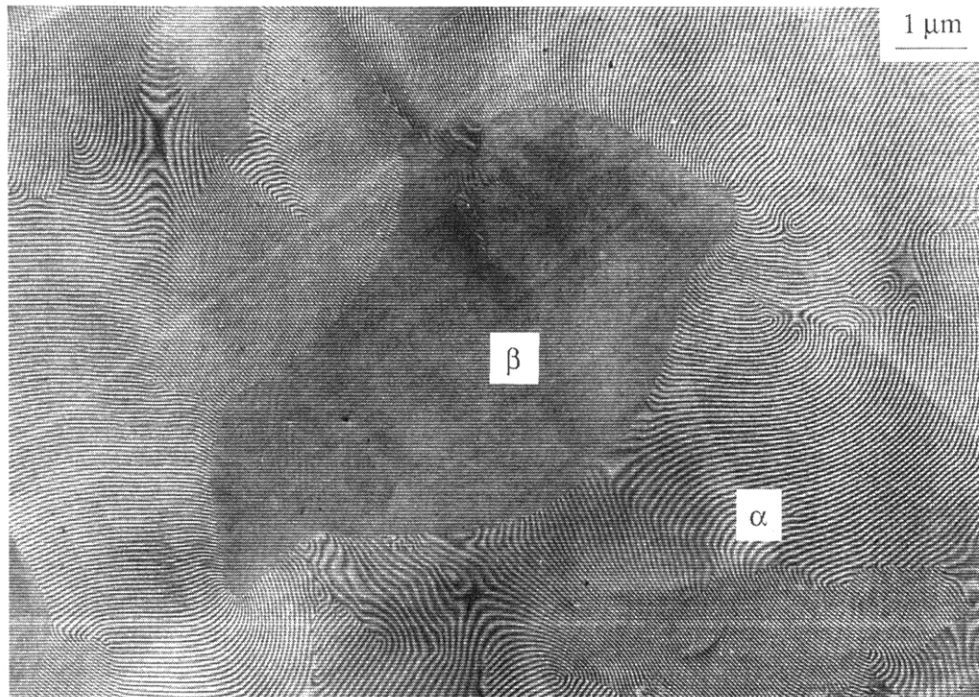


Figure 7. Transmission electron micrograph obtained with a lower magnification than Figure 3 for HY-8/HY-12 50/50 w/w. The matrix is composed of the large lamellar microdomains, and the dispersed phase is composed of the small lamellar microdomains.

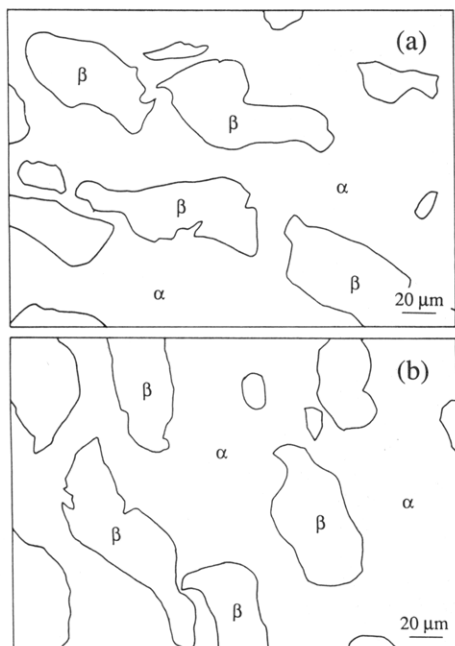


Figure 8. Sketch of two typical TEM micrographs for HY-8/HY-12 50/50 w/w obtained with a lower magnification than that in Figure 7. The sketch highlights the shape of the macroscopic interface between the α -rich and β -rich macrodomains and is obtained by precisely tracing the real macroscopic interface and by ignoring the interfaces of microdomains.

Figure 11 schematically illustrates our interpretation on a possible mechanism on the growth of lamellar microdomains in the ordering process involved by solvent evaporation. This microphase separation is expected to form lamellar microdomains swollen with solvent as schematically shown by the domains with the boundary lines G_1 in the matrix of disordered solution. That is, at a given time in the nucleation process, the matrix, composed of 50/50 w/w mixtures of copolymers α and β , is considered to be not yet transformed to the lamellae and remained in the disordered state. In the beginning of microphase separation, the lamellar domains G_1 are

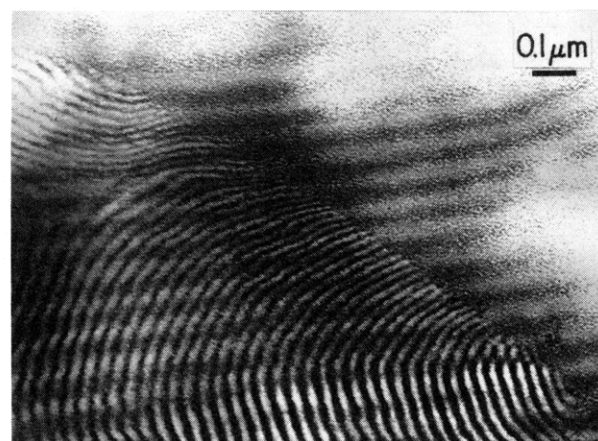


Figure 9. Transmission electron micrograph for HK-17/HS-10 with the composition 80/20. The mixtures show the macrodomains composed of lamellar microdomains rich in copolymers α (HS-10) and those of the disordered phase rich in copolymers β (HK-17).

expected to be composed of 50/50 w/w mixtures of copolymers α and β . This composition is equal to the initial composition of the mixtures.

However, copolymers α can solubilize copolymers β only up to 30% (equal to $1 - \phi_{\alpha,c}^L$) in their lamellar microdomains, according to our experimental results. If this is the case, the excess copolymers β in the domains G_1 should be eventually segregated out from the domains. The lamellar domains G_1 then become rich in copolymers α , having the composition α/β equal to $\phi_{\alpha,c}^L/(1 - \phi_{\alpha,c}^L)$, i.e., 70/30 w/w. As a consequence of this segregation effect, the matrix becomes rich in copolymers β . Since the segregation power between PS and PI block chains is still low for the β -rich matrix phase at c_1 or t_1 , the matrix phase remains in a single-phase state. Therefore, at a given time t_1 or concentration c_1 , we may end up having a system in which the lamellar microdomains G_1 rich in copolymers α are dispersed in the disordered matrix rich in copolymers β . It may be reasonable to consider that the dispersed domains have an ellipsoidal shape with their major axes parallel to the direction of the average orientation of the

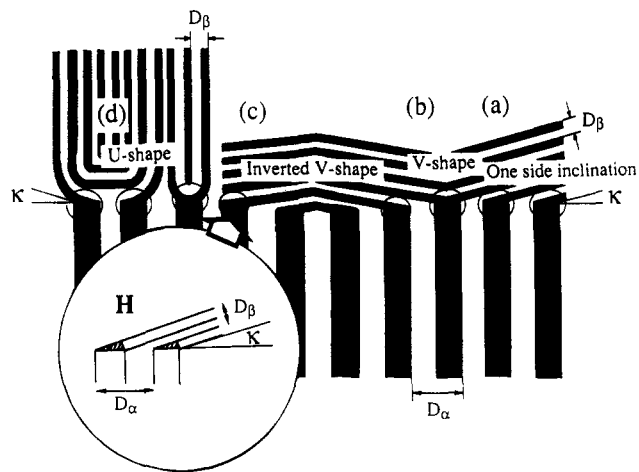


Figure 10. Schematic diagram showing some typical commensurations of thick and thin lamellae at macroscopic interfaces: (a) one-side inclination, (b) V-shape, (c) inverted V-shape, and (d) U-shape.

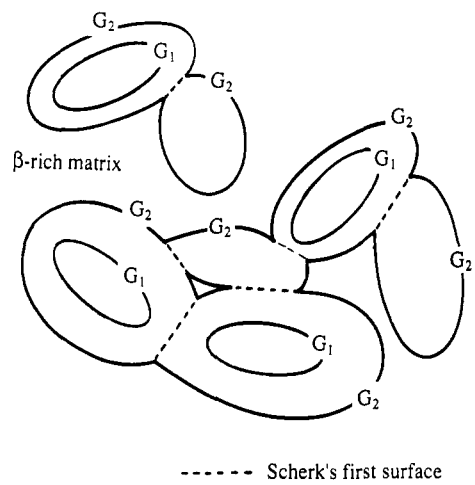


Figure 11. Schematic illustration showing a possible ordering process of the binary mixtures of copolymers α/β with $r = N_\alpha/N_\beta > 10$.

lamellar interfaces, simply because the bending of lamellae has a penalty of free energy increase. The aspect ratio of the domains is a function of the segregation power between PS and PI in solution and hence of the polymer concentration. The volume fraction X of the lamellar domains G_1 depends on the segregation power at c_1 . This X determines the composition of α and β ($\phi_{\alpha,M}$ and $\phi_{\beta,M}$, respectively) in the β -rich phase; $\phi_{\alpha,M} = (0.5 - 0.7X)/(1 - X)$ and $\phi_{\alpha,M}/\phi_{\beta,M} = (5 - 7X)/(5 - 3X)$. If $X = 0.1$, then $\phi_{\alpha,M}/\phi_{\beta,M} = 43/47$, and if $X = 5/7$, then $\phi_{\alpha,M}/\phi_{\beta,M} = 0$. In the latter case the β -rich phase becomes the dispersed phase purely composed of β copolymers.

At a later time t_2 or higher concentration c_2 , the segregation power between A and B block chains increases. Hence, the matrix rich in β copolymers can now form the lamellae. The formation of lamellae occurs anywhere in the matrix, in the middle or in the peripheries of the already existing lamellar microdomains as drawn schematically by the solid lines G_2 . However, newly formed lamellar domains should have a composition of α/β equal to $\phi_{\alpha,M}/\phi_{\beta,M} = (5 - 7X)/(5 - 3X)$ in the beginning of the microphase separation at c_2 . Again an excess amount of β copolymers may be segregated from the newly developed lamellae to end up with lamellae composed of a α/β mixture with a composition of 70/30 w/w. The matrix becomes rich in β as X increases and is left out in the disordered state because the segregation power for this β -rich matrix is not yet sufficient for microphase separation. Toward the end of the solvent evaporation, the β domains may be composed

of almost pure copolymers β . These domains are eventually transformed into lamellae with thickness D_β upon further increase of the concentration c or the segregation power between the PS and PI block chains.

We now consider a possible picture of self-assembly in which the microphase transition starts to occur according to the SD mechanism, instead of the NG mechanism. In this case the lamellar structures may be developed all over the space, with their lamellar normals changing from place to place and hence having macroscopically random orientation. The lamellae initially formed may have a composition of α/β 50/50 as discussed above. However, an excess amount of β copolymers tends to be segregated out from the lamellar phase, due to the segregation effect as discussed above. This effect may produce a number of small disordered domains of β copolymers. These small β domains thus formed remain disordered as the segregation power for this β phase is not sufficient. However, they tend to grow by the diffusion-coalescence mechanism, which is driven by interfacial tension between the disordered β domains and the ordered domains rich in copolymers α . The segregation of β copolymers and the coarsening of β domains promote ordering of α -rich domains. As the concentration or the segregation power of the systems is raised, the domains β are further grown and thin lamellae are eventually formed in the domains as a consequence of microphase separation of copolymers β .

The thin lamellae thus formed should commensurate with preexisting thick lamellae, and the shapes of the thin lamellae domains tend to be controlled by the macrophase separation process between the α -rich lamellar domains and the disordered β -rich domains. The elasticity of the α -rich lamellar domains may cause their shape to be irregular as observed in the TEM micrographs shown in Figures 7 and 8 and as schematically drawn in Figure 11. The orientation variation of the lamellar normals in the α -rich macromodules determines the grain boundary structures via Scherk's first surface. The commensuration of the thin lamellae with the thick lamellae at the macroscopic interface should control the grain boundary structure inside the β domains. The pattern formation occurring in this system seems to be quite analogous to that found in thermotropic liquid crystalline polymer systems¹⁴ when it is transformed from an isotropic melt state to a biphasic state or from a purely nematic state to a biphasic state where liquid crystalline and isotropic phases coexist.

The self-assembly mechanism as described above may explain the important experimental observations, i.e., (i) the irregularity in the shape of the macroscopic interfaces, which results from impingements of the ellipsoidal α -rich domains or from growth of the small but numerous β domains segregated out from the initially formed lamellar domains according to the SD mechanism, and (ii) the β -rich domains dispersed in the matrix of the α -rich domains, as a result of the solubilization criterion of eq 1: the β -rich domains become a minority and hence dispersed phase, because about 30 wt % of β copolymers can be solubilized in the phase composed of copolymers α . The β -rich domains remain in the disordered state in high concentrations and bulk for HK-17/HS-10 because the segregation power of HK-17 is weak, owing to the small DP.

We next consider a qualitative picture of possible models which may account for our experimental results. When the mixture α/β becomes thermodynamically unstable, the plane wave concentration fluctuations are generated. Figure 12a schematically shows a dominant mode of the concentration fluctuations where the wave number q_m may be governed by copolymers α , i.e., q_m may be smaller than

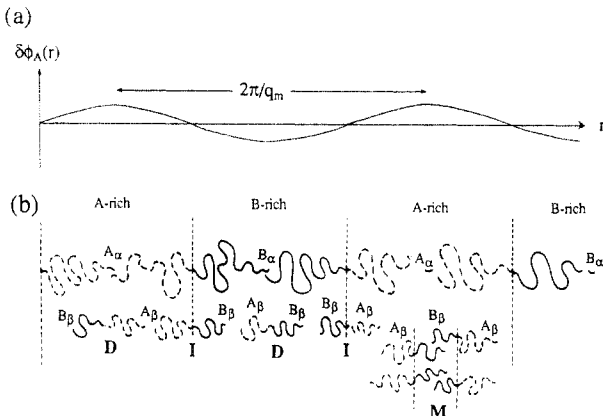


Figure 12. Schematic illustration showing the fluctuation-induced segregation effect: when the concentration fluctuations of the mixtures with $r = N_\alpha/N_\beta > 10$ become large, the small copolymers β may feel as if they were put in the field of homopolymers A_α or B_α .

the q_m for pure copolymers β . These plane wave fluctuations generate the domains rich in A_α and B_α block chains where A_α and B_α are A and B block chains in the α copolymers.

As the amplitudes of the fluctuations increase by further increasing the segregation power beyond the spinodal point into the two-phase region, the small copolymers β , $(A-B)_\beta$ (designate as $A_\beta-B_\beta$ in Figure 12), are put in the field rich in A_α or B_α ; they feel as if they are put in the field of the homopolymers A_α or B_α , as shown in Figure 12b for copolymers labeled **D**. The repulsive interaction between A_α and $(A-B)_\beta$ or B_α and $(A-B)_\beta$ drives (i) the segregation of β copolymers out of the α domains or (ii) the localization of β copolymers at the interface with A_β and B_β block chains confined in A-rich and B-rich domains of α , as shown for the copolymer labeled **I** in Figure 12b or (iii) the micellization into the lamellar domains, as shown by the domains labeled **M** in Figure 12b. Case iii is hardly observed in our TEM observation. Note that our experimental results imply that up to about 30% of copolymers β may be solubilized in state **I** in the solid state. We will denote this segregation effect due to case i or ii as *fluctuation-induced segregation* of copolymers β . We propose that this fluctuation-induced segregation causes the *macrophase separation induced by the microphase separation*.

C. Thermodynamic Stability Analysis and Self-Assembling Mechanism. In the previous section we interpreted the macrophase separation of the block copolymer mixtures α/β on the basis of the *macrophase separation induced by microphase separation*. We analyze here the thermodynamic stability of the mixture in order to investigate whether the mixtures become unstable for a single mode having a wave number q^* or for the double modes having wavenumbers q_1^* and q_2^* , corresponding to the thicker and thinner lamellar micro-domains, for example. The analysis was made in the context of the random-phase approximation (RPA).^{15,16} In applying RPA to our mixtures α/β , we assume that the concentrations fluctuations of segment A in α copolymers, $\delta\phi_{A\alpha}$, and those in β copolymers, $\delta\phi_{A\beta}$, are coupled, as in the earlier work of Leibler and Benoit¹⁷ for the polydisperse A-B block copolymers and of Mori et al.¹⁸ for binary mixtures of block copolymers (see the appendix). It may be general to allow $\delta\phi_{A\alpha}$ and $\delta\phi_{A\beta}$ to be independent variables. This kind of generalized analysis is now in progress in our laboratory.¹⁹ The generalized analysis can be done by considering a special case of mixtures composed of A-B diblock copolymer and C-D diblock copolymers²⁰

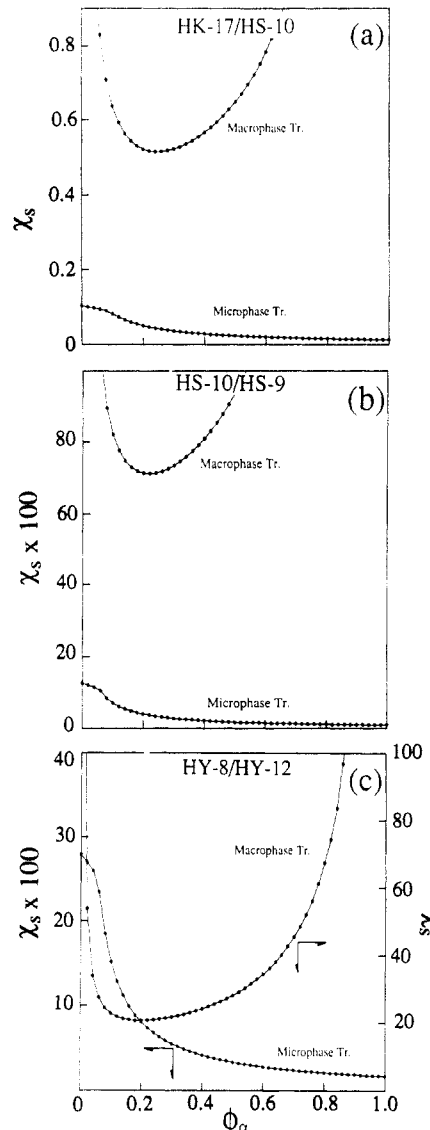


Figure 13. Phase diagrams calculated by RPA, showing the spinodal lines for the macrophase and microphase transitions for the binary mixtures (a) HK-17/HS-10, (b) HS-10/HS-9, and (c) HY-8/HY-12. All diagrams show a relationship of $\chi_{s,\text{micro}} \ll \chi_{s,\text{macro}}$. Thus the stability analysis cannot predict the macrophase transition for these systems. ϕ_α designates the volume fraction of the large molecular weight copolymers in the mixtures.

in which A and B are identical chemically to C and D, respectively.

The thermodynamic force required to generate the q Fourier mode of the thermal fluctuation $F(q)$ was calculated for the block copolymer mixtures α/β having asymmetry in segmental volumes. The detailed final formula for $F(q)$ as well as the parameters used to calculate $F(q)$ will be summarized in the appendix. $F(q)$ is given by

$$F(q) = S(q)/W(q) - 2\chi \sim I^{-1}(q) \quad (3)$$

where $S(q)/W(q)$, defined also in the appendix, is the term which depends only on the conformation of the copolymers and χ is the Flory-Huggins segmental interaction parameter between PS and PI. Obviously $F(q)$ is inversely related to the elastic scattering intensity, $I(q)$. The stability limits (or spinodal points) for the microphase ($\chi_{s,\text{micro}}$) and macrophase ($\chi_{s,\text{macro}}$) transitions were determined from

$$F(q^*) = S(q^*)/W(q^*) - 2\chi_s = 0 \quad (4)$$

where q^* is the Fourier mode which becomes unstable,

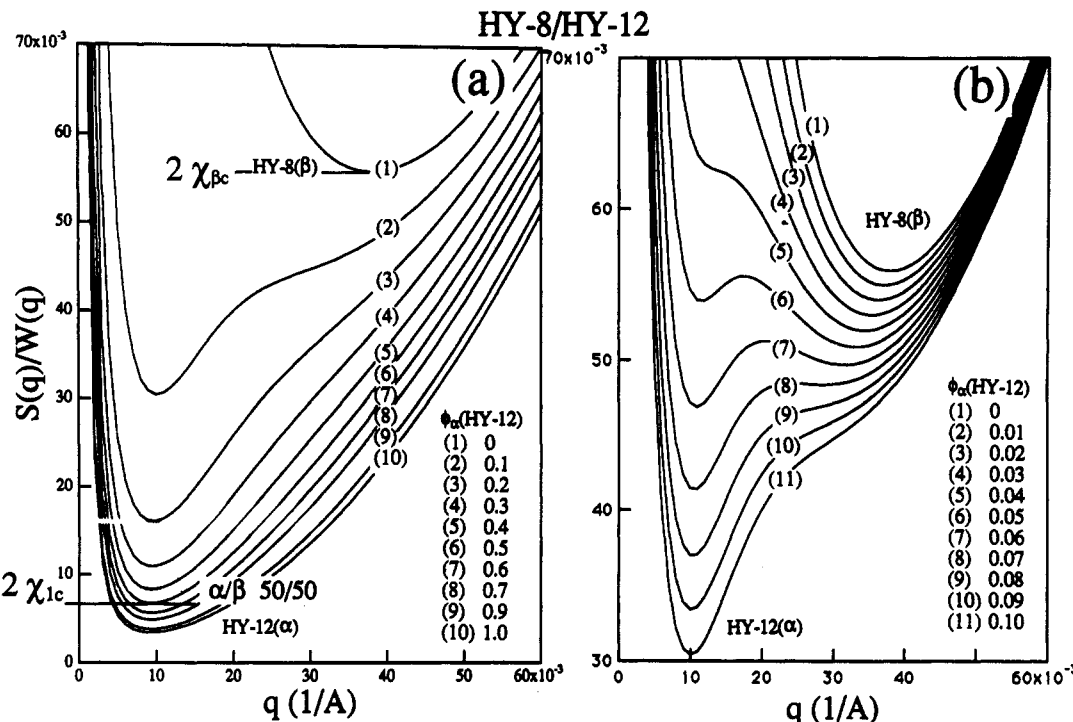


Figure 14. RPA prediction of the thermodynamic force $F(q)$ required to generate the q Fourier mode of the concentration fluctuations when $\chi = 0$ for the binary mixture HY-8/HY-12. The composition of the large molecular weight copolymer ϕ_α is changed from 0 to 1.0 (a) and from 0 to 0.1 (b).

i.e., $\chi_s = \chi_{s,\text{micro}}$ in the case when $q^* \neq 0$ and $\chi_s = \chi_{s,\text{macro}}$ in the case when $q^* = 0$.

Figure 13 shows χ_s for the macrophase transition ($\chi_{s,\text{macro}}$) and the microphase transition ($\chi_{s,\text{micro}}$) for the copolymer mixtures HK-17/HS-10 (a), HS-10/HS-9 (b), and HY-8/HY-12 (c). The results obviously showed

$$\chi_{s,\text{micro}} \ll \chi_{s,\text{macro}} \quad (5)$$

for all the mixtures at all compositions. Thus all the mixtures first become unstable definitely for the microphase transition with increasing the segregation power as a consequence of solvent evaporation or of lowering temperature. After onset of the microphase transition and formation of the microdomains, the spinodal lines for the macrophase transition lose their physical significance. Thus the stability analysis predicts only the microphase transition in the beginning of the ordering process.

Figure 14 shows the thermodynamic force $F(q)$ required to generate the q Fourier mode of the concentration fluctuations at the limit of $\chi = 0$, i.e., $S(q)/W(q)$ for the HY-8/HY-12 mixture with various volume fractions ϕ_α (HY-12); part a shows $S(q)/W(q)$ for ϕ_α from 0 to 1.0, but part b highlights $S(q)/W(q)$ for ϕ_α from 0 to 0.1. Let us now consider a typical mixture having a composition of HY-12 equal to 0.5. This mixture becomes unstable when 2χ increases to $2\chi_{1c}$ shown in part a and the unstable mode has $q = q^* \approx 1 \times 10^{-2}$, the value of which is close to q^* for pure HY-12. When χ increases to a value slightly larger than χ_{1c} , the mixture undergoes microphase separation and may start to generate lamellar domains. In the beginning of microphase separation, the domains are composed of α/β with a 50/50 composition. However, the fluctuation-induced segregation effect may cause the segregation of β copolymers from the domains, giving rise to macrophase separation between the ordered α -rich domains and the disordered β -rich domains, as described earlier in section IV.B. The disordered β domains eventually undergo microphase separation at $\chi \geq \chi_{\beta c}$.

It should be noted that the mixture becomes unstable simultaneously for the two modes q_1^* and q_2^* only for the

very special composition of α/β , close to 0.055/0.945 as shown in part b of Figure 14. The two unstable modes may compete for growth to result in macrophase separation. However, this is not the case of our observation in this work.

V. Concluding Remarks

Binary mixtures of poly(styrene-block-isoprene) (SI) of similar composition, which by themselves form the lamellar microdomains in the segregation limit, were found to exhibit macrophase separation into lamellar domains rich in large molecular weight copolymers and those rich in small molecular weight copolymers, in the case when the two SI copolymers have a molecular weight ratio greater than 10. Macrophase separation was proposed to occur as a consequence of microphase separation. *This macrophase separation induced by microphase separation was proposed to be a consequence of the fluctuation-induced segregation effect discussed in section IV.B (the last paragraph).* This fluctuation-induced segregation effect accounts for our basic experimental observations: (1) macrophase separation, giving rise to the β -rich domains as a minority phase, (2) a miscibility window in composition, and (3) the unique shape of the macrointerface. Various types of commensurations were found in the grain boundaries between the thick and thin lamellae. It is highly required to study *in situ* the self-assembling structures for the copolymer solution as a function of polymer concentration ϕ_α in order to confirm our postulate on the self-assembling mechanism which may lead to macrophase separation induced by microphase separation. Up to this moment the experimental results presented here have not been compared with some theoretical results on the mixtures of block copolymers.⁷ The comparison should be made in the future.

Acknowledgment. This work was supported in part by a Grant-in-Aid for Scientific Research (05650673) from the Ministry of Education, Science and Culture, Japan.

Appendix

Thermodynamic Stability Analysis Based on Random-Phase Approximation. The final formula for $F(q)$ as well as the parameters used to calculate $F(q)$ will be summarized here. $I^{-1}(q) \sim F(q)$ was calculated in the context of the mean-field random-phase approximation (RPA).^{15,16} The intensity of elastic scattering from single block copolymers in the disordered state is given by

$$I^{-1}(q) \sim F(q) = S(q)/W(q) - 2\chi \quad (\text{A-1})$$

where

$$\begin{aligned} S(q) &= S_{AA}(x) + S_{BB}(x) + 2S_{AB}(x) \\ W(q) &= S_{AA}(x)S_{BB}(x) - S_{AB}(x)^2 \\ x &= q^2 R_g^2 = q^2 N \bar{a}^2 / 6 \end{aligned} \quad (\text{A-2})$$

χ is the Flory-Huggins interaction parameter per segment, R_g is the radius of gyration of the block copolymer as a whole, and N is the total degree of polymerization (DP) of a given block copolymer. Here \bar{a} is the average segment length defined by

$$\bar{a} = [fa_A^2 + (1-f)a_B^2]^{1/2} \quad (\text{A-3})$$

where a_A and a_B are the statistical segment lengths of A and B block chains, respectively. The functions $S_{ij}(x)$ ($i, j = A$ or B) are the Fourier transforms of the density-density correlation functions for i and j monomers in a given block copolymer chain which are described by the Debye function, if the chains are ideal.

$$S_{AA}(x) = g(f, x) = (2N/x^2) [fx + \exp(-fx) - 1] \quad (\text{A-4})$$

$S_{BB}(x)$ is given by replacing f in eq A-4 by $1-f$. S_{AB} is given by

$$S_{AB}(x) = (1/2)[g(1, x) - g(f, x) - g(1-f, x)] \quad (\text{A-5})$$

where f is the inner volume fraction of the A block chain in an A-B block copolymer.

For a multicomponent system, the Fourier transform of the density-density correlation function of A monomers was assumed to be given by, after Leibler-Benoit and Mori et al.^{17,18}

$$\begin{aligned} S_{AA}(x) &= \sum_m \phi_m S_{AAm}(x_m) \\ x_m &= q^2 R_{gm}^2 = q^2 N_m \bar{a}_m^2 / 6 \end{aligned} \quad (\text{A-6})$$

where N_m and ϕ_m are the total DP and fraction of A in the m th A-B block copolymer, respectively. For our binary mixtures of A-B block copolymers, m corresponds to the α and β copolymers, S_{AAm} is the Fourier transform of the density-density correlation function between the two monomers in the m th copolymer. Similarly

$$S_{BB}(x) = \sum_m \phi_m S_{BBm}(x_m) \quad (\text{A-7})$$

$$S_{AB}(x) = \sum_m \phi_m S_{ABm}(x_m) \quad (\text{A-8})$$

For binary copolymer mixtures, the summation in eqs A-6-A-8 has to be done for two kinds of copolymers, α and β . Here we assumed that concentration fluctuations of the A segment in α copolymers, $\delta\phi_{A\alpha}$, and those in β copolymers, $\delta\phi_{B\beta}$, are coupled to each other and indistinguishable. In general, $\delta\phi_{A\alpha}$ and $\delta\phi_{B\beta}$ should be treated as independent variables.¹⁹

The results shown in Figures 13 and 14 were calculated using the values shown in Table 1 for r_{PS} and r_{PI} for DP of the PS and PI block chains, respectively, and $a_{PS} = 0.707$ nm and $a_{PI} = 0.593$ nm for the statistical segment lengths of the PS and PI block chains, respectively. The block copolymers were assumed to have no polydispersity in their molecular weights.

References and Notes

- (1) Tanaka, H.; Hashimoto, T. *Polym. Commun.* 1988, 29, 212. Hashimoto, T.; Tanaka, H.; Hasegawa, H. In *Molecular Conformation and Dynamics of Macromolecules in Condensed Systems*; Nagasawa, M., Ed.; Elsevier: Amsterdam, The Netherlands, 1988; p 257. Hashimoto, T.; Kimishima, K.; Hasegawa, H. *Macromolecules* 1991, 24, 5704. Hashimoto, T. In *Materials Science and Technology. Vol. 12. Structure and Properties of Polymers*; Cahn, R. W., Haasen, P., Kramer, E. J., Eds.; VCH: Weinheim, Germany, 1993; Chapter 6.
- (2) Hashimoto, T.; Yamasaki, K.; Koizumi, S.; Hasegawa, H. *Macromolecules* 1993, 26, 2895 and references cited therein.
- (3) Helfand, E. *Macromolecules* 1975, 8, 552.
- (4) Helfand, E., Wasserman, Z. R. *Macromolecules* 1976, 9, 879.
- (5) Meier, D. J. In *Thermoplastic Elastomers*; Legge, N. R., Holden, G., Schroeder, H., Eds.; Hanser: Munich, 1987; Chapter 11.
- (6) Milner, S. T.; Witten, T. A.; Cates, M. E. *Europhys. Lett.* 1988, 50, 413. Milner, S. T.; Witten, T. A.; Cates, M. E. *Macromolecules* 1988, 21, 2610. Milner, S. T.; Witten, T. A.; Cates, M. E. *Macromolecules* 1989, 22, 853.
- (7) Birshtein, T. M.; Lyatskaya, Yu. V.; Zhulina, E. B. *Polymer* 1990, 31, 2185. Zhulina, E. B.; Birshtein, T. M. *Polymer* 1991, 32, 1299. Zhulina, E. B.; Lyatskaya, Yu. V.; Birshtein, T. M. *Polymer* 1992, 33, 332. Lyatskaya, Yu. V.; Zhulina, E. B.; Birshtein, T. M. *Polymer* 1992, 33, 343. Birshtein, T. M.; Lyatskaya, Yu. V.; Zhulina, E. B. *Polymer* 1992, 33, 2751.
- (8) Nitsche, J. C. C. *Lectures on Minimal Surfaces Vol. 1*; Cambridge University Press: Cambridge, U.K., 1989. Thomas, E. L.; Alward, D. B.; Henkee, C. S.; Hoffman, D. *Nature* 1988, 334, 598.
- (9) Nishikawa, Y.; Kawada, Y.; Hasegawa, H.; Hashimoto, T. *Acta Polym.* 1993, 44, 247.
- (10) Nishikawa, Y.; Hasegawa, H.; Hashimoto, T.; Hyde, S. T., to be published.
- (11) Mori, K.; Hasegawa, H.; Hashimoto, T. *Polym. J.* 1985, 17, 799.
- (12) Fredrickson, G. H.; Binder, K. *J. Chem. Phys.* 1989, 91, 7265.
- (13) Hashimoto, T. *Macromolecules* 1987, 20, 465.
- (14) Hashimoto, T.; et al., unpublished results.
- (15) de Gennes, P.-G. *Scaling Concepts in Polymer Physics*; Cornell University Press: Ithaca, NY, 1979.
- (16) Leibler, L. *Macromolecules* 1980, 13, 1602.
- (17) Leibler, L.; Benoit, H. *Polymer* 1981, 22, 195.
- (18) Mori, K.; Tanaka, H.; Hashimoto, T. *Macromolecules* 1987, 20, 381.
- (19) Tanaka, F.; Koizumi, S.; Hashimoto, T., in preparation.
- (20) Kim, J. K.; Kimishima, K.; Hashimoto, T. *Macromolecules* 1993, 26, 125.